

## Rotational Motion in LiBH<sub>4</sub>/LiI Solid Solutions

Pascal Martelli,<sup>\*,†,‡</sup> Arndt Remhof,<sup>†</sup> Andreas Borgschulte,<sup>†</sup> Ralf Ackermann,<sup>§</sup> Thierry Strässle,<sup>§</sup>  
Jan Peter Embs,<sup>§</sup> Matthias Ernst,<sup>||</sup> Motoaki Matsuo,<sup>⊥</sup> Shin-Ichi Orimo,<sup>⊥</sup> and Andreas Züttel<sup>†,‡</sup>

<sup>†</sup>Empa Swiss Federal Laboratories for Materials Science and Technology, Hydrogen & Energy, 8600 Dübendorf, Switzerland

<sup>‡</sup>Physics Department, University of Fribourg, 1700 Fribourg, Switzerland

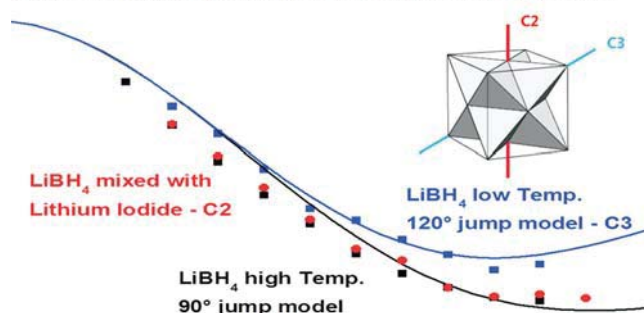
<sup>§</sup>Laboratory for Neutron Scattering, Paul Scherrer Institut, 5232 Villigen PSI, Switzerland

<sup>||</sup>Inorganic Chemistry, ETH Zürich, 8093 Zürich, Switzerland

<sup>⊥</sup>Institute for Materials Research, Tohoku University, Sendai 980-8577, Japan

**ABSTRACT:** We investigated the localized rotational diffusion of the (BH<sub>4</sub>)<sup>-</sup> anions in LiBH<sub>4</sub>/LiI solid solutions by means of quasielastic and inelastic neutron scattering. The (BH<sub>4</sub>)<sup>-</sup> motions are thermally activated and characterized by activation energies in the order of 40 meV. Typical dwell times between jumps are in the picosecond range at temperatures of about 200 K. The motion is dominated by 90° reorientations around the 4-fold symmetry axis of the tetrahedrally shaped (BH<sub>4</sub>)<sup>-</sup> ions. As compared to the pure system, the presence of iodide markedly reduces activation energies and increases the rotational frequencies by more than a factor of 100. The addition of iodide lowers the transition temperature, stabilizing the disordered high temperature phase well below room temperature.

### EISF- Elastic Incoherent Structure Factor



## I. INTRODUCTION

Because of its high hydrogen content,<sup>1</sup> lithium borohydride (LiBH<sub>4</sub>) is the focus of many research activities worldwide. LiBH<sub>4</sub> is an ionic crystal, consisting of (Li)<sup>+</sup> cations and (BH<sub>4</sub>)<sup>-</sup> anions.<sup>2</sup> It undergoes a structural phase transition at 380 K from the ordered low temperature (LT) orthorhombic (*Pnma*)<sup>3,4</sup> phase to the disordered high temperature (HT) hexagonal phase (*P63cm*).<sup>5</sup> The dynamic disorder of the HT phase originates from thermally activated rotational jumps of the (BH<sub>4</sub>)<sup>-</sup> anions in the terahertz range.<sup>6</sup> The structural phase transition is accompanied by a remarkable increase of Li-ion mobility, leading to an increase in (Li)<sup>+</sup> ionic conductivity by more than 3 orders of magnitude from 10<sup>-8</sup> to 10<sup>-5</sup> cm<sup>2</sup>/s.<sup>7-9</sup> The corresponding diffusivities can be obtained via the Nernst–Einstein equation to  $D = 8 \times 10^{-11}$  cm<sup>2</sup>/s<sup>10</sup> in the HT phase at 400 K and to  $D = 1 \times 10^{-13}$  cm<sup>2</sup>/s<sup>7</sup> in the LT phase at 300 K. High Li-ion conductivity has also been reported from other ionic crystals with complex anions such as (SO<sub>4</sub>)<sup>2-</sup> or (ClO)<sup>-</sup>. As for LiBH<sub>4</sub>, these compounds undergo structural phase transitions, and the fast ion conductivity only occurs in the HT phase. In Li<sub>2</sub>SO<sub>4</sub> and Li<sub>3</sub>PO<sub>4</sub>, which are also Li-ion conductors in their respective HT phases, the rotation of the anion is believed to support the cation diffusion by the so-called “paddle wheel mechanism”.<sup>11,12</sup> However, this interpretation is not without controversy, and the validity of the paddle wheel mechanism is under discussion. Other effects such as volume or symmetry changes may be the key factors for both the enhanced diffusivity of the metal as well as the increase in the rotational motion.<sup>13,14</sup> At present, it is unclear whether there is a

causal connection between the ion conductivity and the (BH<sub>4</sub>)<sup>-</sup> rotation in LiBH<sub>4</sub> or not.<sup>15</sup>

The HT phase of LiBH<sub>4</sub> can be stabilized by addition of lithium halides, resulting in the enhanced conductivity at room temperature (RT).<sup>7</sup> The stabilizing effect increases with the size of the halide ion. Already substoichiometric amounts of LiI (<20 mass %) shift the transition temperature well below room temperature. Thereby, the (Li)<sup>+</sup> mobility in LiI at room temperature is rather low, comparable to the one in LT phase of LiBH<sub>4</sub>.<sup>8,16,17</sup>

In the present Article, we examine the effect of the iodide stabilization in LiBH<sub>4</sub>/LiI solid solutions on the rotational motion of the (BH<sub>4</sub>)<sup>-</sup> anions. We identify the axes of rotation, the jump frequencies, and the activation energies by means of quasielastic neutron scattering (QENS). The experimental results are discussed on the basis of the structural properties of the solid solution and are related to the ion mobility.

## II. EXPERIMENTAL METHODS

The samples were prepared from mixtures of powders of Li<sup>11</sup>BH<sub>4</sub> (KatChem) and LiI (Sigma Aldrich), following Oguchi et al.'s recipe.<sup>18</sup> To avoid the strong neutron absorption of <sup>10</sup>B, present in natural boron, <sup>11</sup>B enriched (99 mass %) LiBH<sub>4</sub> was used. About one cubic centimeter of the mixtures with molar ratios of 1:1, 2:1, and 4:1 have been mechanically ball milled during 5 h under Ar

atmosphere. The samples were protected from ambient air and always handled in glove boxes filled with purified argon or helium. Milling was carried out in a gastight container, filled, and sealed within the glovebox.

The state and the purity of the as-milled samples were verified by X-ray diffraction (XRD). Representative samples are measured in glass capillaries (diameter 1 mm, wall thickness 0.01 mm), sealed under argon atmosphere. The X-ray diffraction patterns presented in this work are measured using a Bruker D8 diffractometer, equipped with a Vantec-1 detector and Goebel mirror, selecting Cu  $K_{\alpha}$  radiation with a wavelength of  $\lambda = 1.542 \text{ \AA}$  (weighted average of Cu  $K_{\alpha 1}$  and Cu  $K_{\alpha 2}$  radiation).

Static  $^7\text{Li}$  nuclear magnetic resonance (NMR) spectra with proton decoupling were obtained on a Bruker DMX 400 spectrometer operated at the  $^7\text{Li}$  resonance frequency of 155.5 MHz at an applied magnetic field of 9.39 T. Aqueous LiCl (1 M) was used as the  $^7\text{Li}$  reference.

The quasielastic and the inelastic neutron scattering (QENS and INS) measurements were carried out using the cold neutron time-of-flight (TOF) neutron spectrometer FOCUS located at the continuous spallation source SINQ at the Paul Scherrer Institute, PSI, Switzerland.<sup>19,20</sup>

QENS is a powerful tool to observe hydrogen dynamics<sup>21,22</sup> and has recently been used to study the hydrogen mobility in solid and liquid borohydride.<sup>6,17,23,24</sup>

For these experiments, we used neutrons with an incident wavelength of  $\lambda_i = 4 \text{ \AA}$ , corresponding to an energy of 5.11 meV and resolution of  $\Delta E \approx 0.2 \text{ meV}$  at the elastic line. The samples were loaded in lead sealed, double walled-hollow cylindrical containers. The diameter of the cylindrical container was 10 mm, and the wall distance (i.e., the sample space) was 1 mm. A packing density of about 30% was achieved, resulting in a transparency  $>70 \text{ mass \%}$  for all three samples. The inelastic data from the neutron energy gain side were used to determine the hydrogen partial density of states (PDOS). To obtain the PDOS from the inelastic spectra, the TOF data were corrected for the  $1/\omega$  term, the polarization factor, and the Bose–Einstein statistics for the thermal population. The quasielastic signal was used to gain information on the localized motion of the  $(\text{BH}_4)^-$  subunits in the samples. Data acquisition and treatment were carried out as described in our earlier work.<sup>6</sup> The samples were first heated to the maximum temperature used (400 K) and subsequently cooled. The temperature was then reduced stepwise to 100 K.

### III. RESULTS

**a. Structural Characterization.** Figure 1 compares the measured diffraction patterns for  $4\text{LiBH}_4 + \text{LiI}$  (top red),  $2\text{LiBH}_4 + \text{LiI}$  (middle blue), and  $\text{LiBH}_4 + \text{LiI}$  (bottom green). The measured data (points) are superimposed by structural refinements, based on the structural model of the high temperature phase of  $\text{LiBH}_4$  as reported by Hartman et al.<sup>4</sup> We observe the HT phase for all three samples at RT. The measured lattice parameters are in agreement with Oguchi et al.<sup>18</sup> and Filinchuk et al.<sup>25</sup> No impurities, especially no traces of the original phases, the LT phase of  $\text{LiBH}_4$ , or LiI, are visible, indicating the successful formation of the solid solution. The ticks at the bottom of the figure mark the positions of the HT  $\text{LiBH}_4$  reflections according to Hartman’s model. The shift in the alignment between the ticks and the measured reflections, especially at higher angles, originates mainly due to thermal expansion. The reference data describe the HT phase at 400 K, while the data in this work were recorded at RT. Furthermore, as was observed before,<sup>18</sup> as the

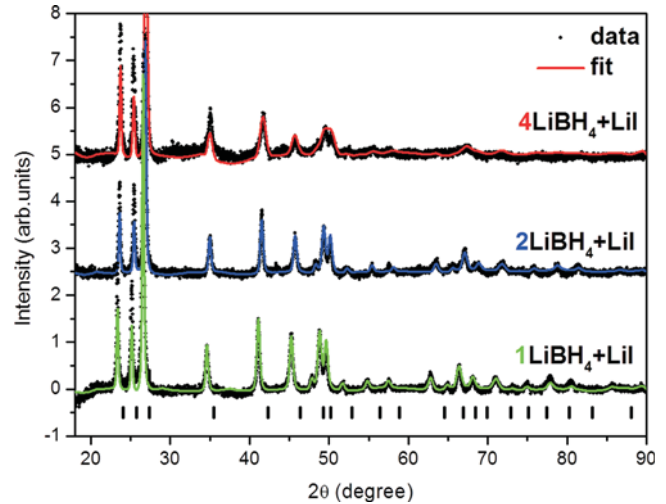


**Figure 1.** Rietveld refined powder XRD profiles of  $x\text{LiBH}_4 + \text{LiI}$  ( $x = 1, 2, 4$ ) at room temperature. The diffraction peaks of the HT (hexagonal) phase of  $\text{LiBH}_4$  are shown at the bottom. No impurities and no LiI have been identified.

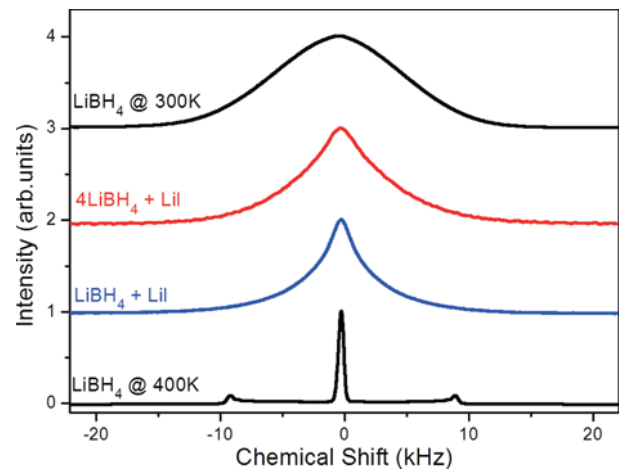


**Figure 2.** Static  $^7\text{Li}$  NMR spectra of pure  $\text{LiBH}_4$ , of  $4\text{LiBH}_4 + \text{LiI}$ , and of  $\text{LiBH}_4 + \text{LiI}$ , all recorded at 300 K, together with a HT spectrum of pure  $\text{LiBH}_4$  recorded at 400 K (from top to bottom).

LiI concentration increases, the lattice constant of solid solution increases, and therefore a slight XRD peak shift to higher angles is observable. The signal/noise ratio of the high angle reflections increases with increasing iodide content. We attribute this to the higher number of electrons, resulting in a higher scattering cross section of the iodine as compared to the borohydride ion.

Figure 2 displays (from top to bottom) the static  $^7\text{Li}$  NMR spectra of pure  $\text{LiBH}_4$ , of  $4\text{LiBH}_4 + \text{LiI}$ , and of  $\text{LiBH}_4 + \text{LiI}$ , all recorded at 300 K, together with a HT spectrum of pure  $\text{LiBH}_4$  recorded at 400 K. In  $\text{LiBH}_4$ , the phase transition is accompanied by an increase in Li-mobility, leading to a motional narrowing of the resonance line.<sup>8,26</sup> A comparison of the 300 K spectra of  $\text{LiBH}_4$  and the  $\text{LiBH}_4/\text{LiI}$  solid solutions shows a considerable narrowing with increasing iodide concentration. The narrowing may result from (i) motional narrowing, resulting from an increased  $(\text{Li})^+$  mobility, or (ii) reduced dipolar coupling to the protons due to the dilution of the  $(\text{BH}_4)^-$  ions by  $(\text{I})^-$ . To

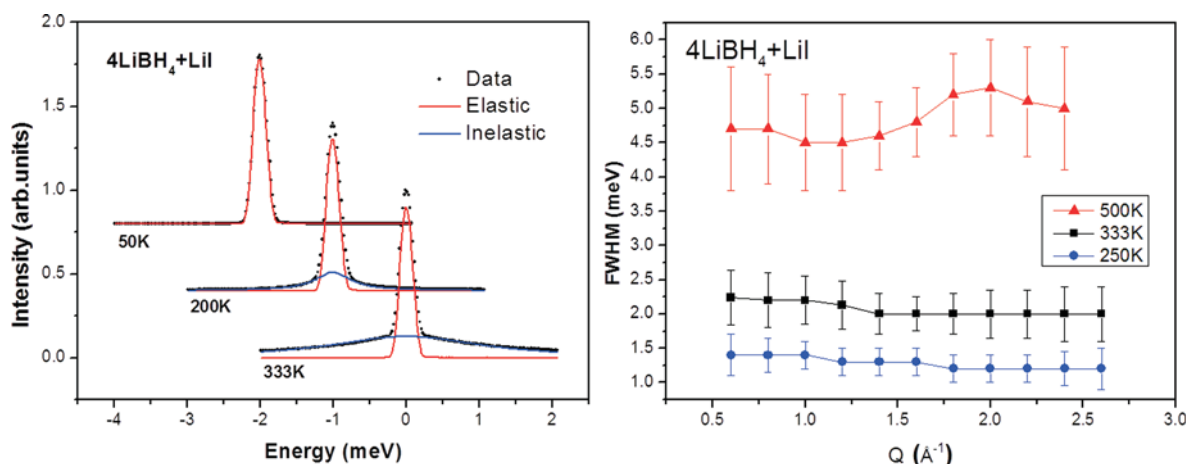


**Figure 3.** Left panel: Representative QENS spectra of  $4\text{LiBH}_4 + \text{LiI}$ , measured at  $T = 50\text{ K}$  (top), at  $T = 200\text{ K}$  (middle), and at  $T = 333\text{ K}$  (bottom). The measured data are represented by black symbols. The measured spectra can be represented by a resolution limited Delta function (red) and a single Lorentzian profile (blue). The spectra are offset for clarity. Right panel:  $Q$ -dependence of the width ( $w_{qe}$ ) of spectra. The error bars were estimated from the fitting of the Lorentzian curve.

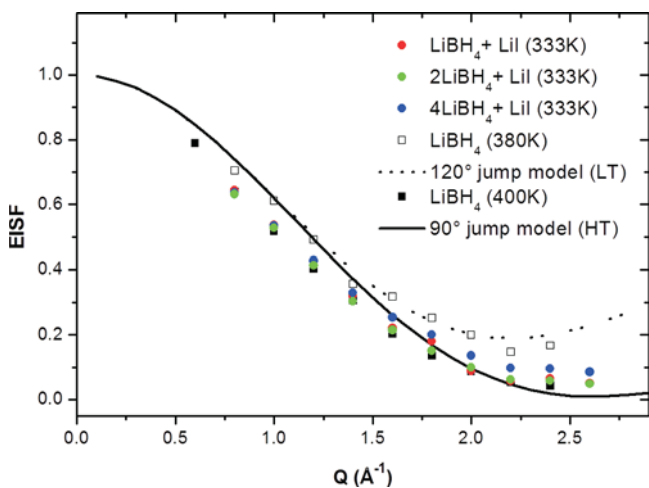


**Figure 4.** EISFs of  $4\text{LiBH}_4 + \text{LiI}$  (blue),  $2\text{LiBH}_4 + \text{LiI}$  (green), and  $\text{LiBH}_4 + \text{LiI}$  (red) measured at  $333\text{ K}$ . Lines represent models of EISF:  $90^\circ$  reorientations about the  $c_2$  axis (dotted line), and a three jump model, involving  $120^\circ$  rotations about the  $c_3$  axis (straight line), respectively. For comparison, the measured EISFs for the HT and the LT phase of pure  $\text{LiBH}_4$ , measured at  $400$  and  $380\text{ K}$ , are plotted as well.

avoid the dilution effect, the measurements have been measured in a proton decoupled mode. This narrowing results from the increased  $(\text{Li})^+$  mobility in the iodide stabilized HT phase.<sup>7</sup> We therefore confirm (i) the structural stabilization of the HT phase as well as (ii) the increased  $(\text{Li})^+$  mobility of the  $\text{LiBH}_4/\text{LiI}$  solid solution as compared to the pure system.

**b. Quasielastic Neutron Scattering.** For all samples under investigation, no broadening of the elastic line was found for temperatures below  $100\text{ K}$ , showing that the hydrogen is frozen on the time scale accessible by the instrument. At higher temperatures, a quasielastic broadening is observed, whose width increases with temperature. Figure 3 (left panel) displays three representative QENS spectra of  $4\text{LiBH}_4 + \text{LiI}$ , recorded at  $50$ ,  $200$ , and  $333\text{ K}$  (black symbols), deconvoluted in the resolution limited elastic line (blue) and the quasielastic broadening (red). The spectra are offset for clarity. All QENS spectra were modeled

using two components: first, the elastic peak of width  $w_{el}$  and an integrated area  $I_{el}$ . The width of the elastic line was fixed to the width of the measured elastic line of a vanadium standard sample, corresponding to the instrumental resolution. Second, the quasielastic broadening was modeled by a single Lorentzian curve with a width  $w_{qe}$  and an integrated area  $I_{qe}$ . In all fits, the peak centers were constrained to be the same for each component. Selected spectra were binned in a range of momentum transfer of  $Q = 0.6 - 2.6\text{ \AA}^{-1}$  with bin width of  $0.2\text{ \AA}^{-1}$ . As for pure monovalent alkali metal borohydrides, at a given temperature, the quasielastic broadening is independent of  $Q$  (Figure 3, right panel) as discussed in detail in refs 6 and 27, indicative of a localized hydrogen motion.

The rotational behavior of the  $(\text{BH}_4)^-$  units can be described on the basis of their elastic incoherent scattering factors (EISFs).<sup>28,29</sup> Figure 4 displays experimentally obtained EISFs, extracted from the QENS spectra recorded at  $333\text{ K}$  according to  $\text{EISF} = I_{el}(Q)/(I_{el}(Q) + I_{qe}(Q))$  together with model EISFs describing (i)  $90^\circ$  reorientations of the  $(\text{BH}_4)^-$  as observed in the HT phase of  $\text{LiBH}_4$  (straight line) and (ii)  $120^\circ$  rotational jumps as found in the LT phase (dotted line).<sup>6</sup> For comparison, the data for pure  $\text{LiBH}_4$  in the respective phases were added to the graph. For all temperatures and for all iodine concentration, the reorientational model involving  $90^\circ$  jumps about the three perpendicular  $c_2$  axis best describes the measured data. We attribute the deviation of the EISF data from the models, especially at low  $Q$ , to multiple scattering effects. Within the accuracy of the measurement, no influence of the iodine contents could be detected. We therefore conclude that the  $(\text{BH}_4)^-$  units within the iodide stabilized HT phase of  $\text{LiBH}_4$  undergo  $90^\circ$  reorientational jumps, similar to the HT phase of the pure material.

The iodine content does not obviously change the axis of rotation. It does, however, influence the frequency (and therefore the dwell time) of the rotational motion. Figure 5 compares the QENS of pure  $\text{LiBH}_4$ , of  $4\text{LiBH}_4 + \text{LiI}$ , of  $2\text{LiBH}_4 + \text{LiI}$ , and of  $\text{LiBH}_4 + \text{LiI}$ , recorded at  $400\text{ K}$ . As the quasielastic linewidths are independent of  $Q$  (see Figure 3), the spectra were not binned in different  $Q$ -groups. Figure 5 displays therefore an average over all momentum transfers. Superimposed to the measured data (black), the quasielastic component (red) is shown.

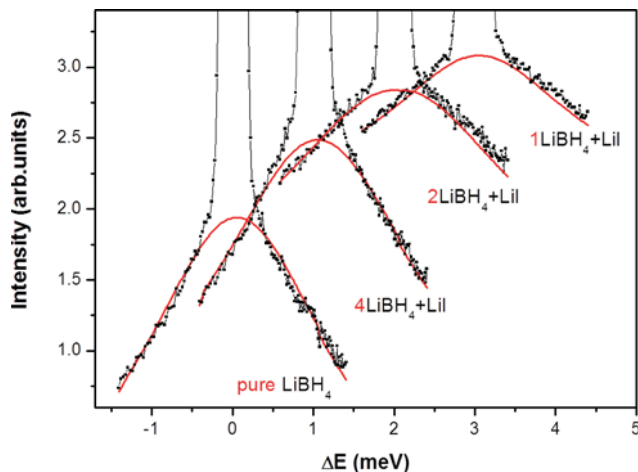


**Figure 5.** QENS spectra of pure  $\text{LiBH}_4$  and solid solutions of  $\text{LiBH}_4$  and  $\text{LiI}$ , recorded at 400 K. A broadening effect is observable; the mobility increases with the amount of  $\text{LiI}$ . To increase the statistics, the spectra were not separated in different  $Q$ -groups.

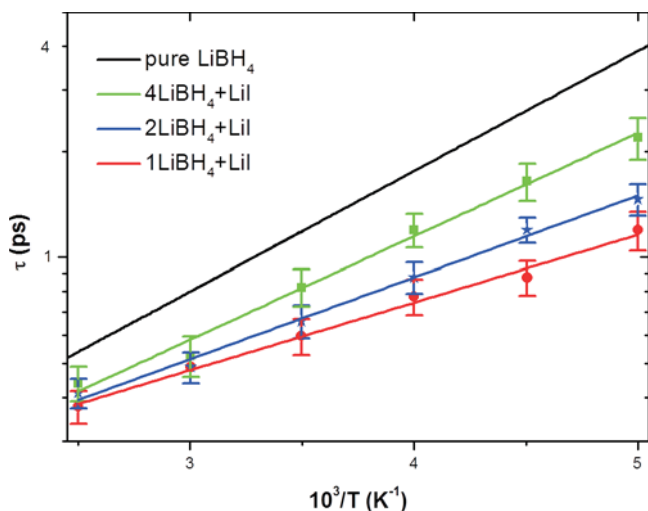


**Figure 6.** Thermally activated Arrhenius behavior of the rotational motion. The time  $\tau$  corresponding to the inverse width of the quasielastic broadening can be expressed as  $\tau = \tau_0 \exp(E_a/k_B T)$ .

The spectra are offset for clarity. It can be clearly seen that  $w_{qe}$  increases steadily with increasing iodine content. A comparison with the pure system<sup>6</sup> shows that at 400 K the  $\text{LiBH}_4/\text{LiI}$  solid solution exhibits the same quasielastic broadening and thus the same dwell time as pure  $\text{LiBH}_4$  at 500 K.

Obviously, in the  $\text{LiBH}_4/\text{LiI}$  solid solutions the  $(\text{BH}_4)^-$  units display enhanced rotational dynamics.<sup>30</sup> The temperature dependence of the broadening follows the Arrhenius law. As described previously,<sup>6</sup>  $w_{qe}$  can be related to the average dwell time  $\tau$ , which can be expressed as  $\tau = \tau_0 \exp(E_a/k_B T)$ , where  $E_a$  is the activation energy,  $\tau_0$  is the inverse attempt frequency,  $T$  is the temperature, and  $k_B$  is Boltzmann's constant. Figure 6 shows the experimentally obtained data together with the Arrhenius fits in the temperature range from 200 to 400 K. Green squares represent the 4:1 sample, blue stars the 2:1 sample, and red dots the 1:1 sample. The error bars represent the scatter of the widths of the Lorentzian contributions around their respective mean

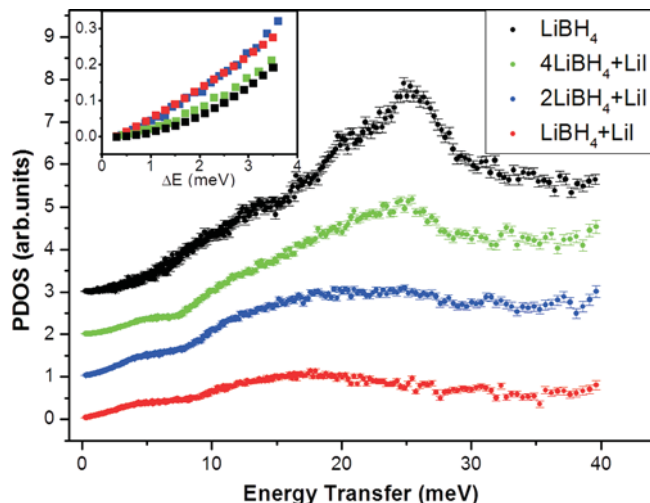


**Figure 7.** From bottom to top: Measured PDOS of  $\text{LiBH}_4 + \text{LiI}$ , of  $2\text{LiBH}_4 + \text{LiI}$ , of  $4\text{LiBH}_4 + \text{LiI}$  (all measured at 100 K), and of pure  $\text{LiBH}_4$ , recorded in a previous experiment at 200 K. Data are corrected for the  $1/\omega$  term, the polarization factor, and the Bose–Einstein statistics for the thermal population. The spectra are normalized to monitor counts. The data are offset for clarity.

value. The black line is an extrapolation of the HT behavior ( $E_a = 68$  meV and  $\tau_0 = 75$  fs) to lower temperatures.<sup>6</sup> For all temperatures, the activation energies become shorter with increasing iodine content. Fits to the data yield  $E_a = 58 \pm 4$  meV and  $\tau_0 = 76 \pm 5$  fs for the 4:1 sample,  $E_a = 46 \pm 3$  meV and  $\tau_0 = 103 \pm 5$  fs for the 2:1 sample, and  $E_a = 38 \pm 3$  meV and  $\tau_0 = 126 \pm 4$  fs for the 1:1 sample, respectively. The accuracy of the values for the activation energies and the prefactors result from the error bars of the individual data points and the relatively small temperature range of 200 K. We cannot exclude a certain deviation of the jump rates of individual  $(\text{BH}_4)^-$  ions from the average one due to the disordered nature of the solid solution.

**c. Inelastic Neutron Scattering.** While the quasielastic part of the spectra yields information about the stochastic motion of single particles, the inelastic spectra measure collective motions. Because of the large incoherent-scattering cross section of hydrogen, mainly the hydrogen partial phonon density of states (PDOS) is measured. Figure 7 displays from bottom to top the measured PDOS of  $\text{LiBH}_4 + \text{LiI}$ , of  $2\text{LiBH}_4 + \text{LiI}$ , of  $4\text{LiBH}_4 + \text{LiI}$  (all measured at 100 K), and of pure  $\text{LiBH}_4$ , recorded in a previous experiment at 200 K. The spectra are offset for clarity. The dominating peaks of the translatory optic modes, which are clearly visible around 25 meV in the spectrum of the pure  $\text{LiBH}_4$ ,<sup>31</sup> broaden and shift to lower energies with increasing iodine content, which we mainly attribute to the increasing average anion mass with increasing  $\text{LiI}$  content. As compared to the thermal behavior of pure  $\text{LiBH}_4$ <sup>3</sup> and of pure  $\text{KBH}_4$ ,<sup>6</sup> the addition of iodine has qualitatively the same effect as a temperature increase. The broadening of the peak with increasing temperature can be explained by a reduced correlation length.

In the energy range below 5 meV, the addition of iodine results in a change of the slope of the PDOS. At low temperatures and at low energies, the PDOS of pure alkali metal borohydrides depends quadratically on the phonon energy as expected by the Debye theory for acoustic modes in crystalline solids. Also, the  $4\text{LiBH}_4 + \text{LiI}$  sample behaves in this way, similar to pure  $\text{LiBH}_4$ . With increasing iodine content, the slope changes and

approaches a linear behavior. Again, the same effect has been observed in pure  $\text{LiBH}_4$ <sup>3</sup> and in pure  $\text{KBH}_4$ <sup>6</sup> at higher temperatures. The excess of low-energy density of states, as compared to the Debye behavior, reveals lattice anharmonicities and is a characteristic feature of glasses and disordered systems.<sup>32,33</sup> For the pure borohydrides, the increasing disorder was attributed to the enhanced rotational motion with increasing temperature. Obviously, iodide addition has the same effect.

#### IV. DISCUSSION

The localized motion of the  $(\text{BH}_4)^-$  ions in the alkali metal borohydrides can be described as a hindered rotor state, in which the anion undergoes librations in a harmonic potential and eventually makes a rotational jump. The  $\text{LiBH}_4/\text{LiI}$  solid solutions show lower activation energies and shorter dwell times as the  $(\text{I})^-$  concentration increases. At room temperature, the jump frequency is in the terahertz regime with activation energies in the order of 50 meV. Thus, the addition of  $(\text{I})^-$  has qualitatively the same effect as a temperature increase.

Miyazaki et al. observed the same behavior for the  $(\text{Li})^+$  ion conductivity in these systems. The conductivity of  $\text{LiBH}_4/\text{LiI}$  solid solutions increases with increasing LiI content.<sup>16</sup>

There are indications that the disorder resulting in the HT-phase of  $\text{LiBH}_4$  is induced by the increasing mobility (delocalization) of  $(\text{Li})^+$ -atoms below the phase transition temperature,<sup>34</sup> confirming results from first-principles molecular dynamics simulations.<sup>35</sup> As  $\text{LiBH}_4$  contracts during the phase transition (from LT to the HT phase), a stabilization of the HT phase by replacing the  $(\text{BH}_4)^-$  ion with the smaller  $(\text{Cl})^-$  ion<sup>7,36</sup> is reasonable, as the smaller  $(\text{Cl})^-$  ion favors the denser structure. The stabilizing effect of the larger  $(\text{Br})^-$  and  $(\text{I})^-$  is counterintuitive and cannot be understood on the basis of the lattice contraction. Furthermore, the stabilizing effect is stronger the bigger is the ionic radius of the halide ion replacing the  $(\text{BH}_4)^-$  ion.

By first principles molecular dynamics calculations, Ikeshoji et al. explained the Li fast ion conductivity in the HT phase of  $\text{LiBH}_4$  by the diffuse and doubly split atom occupation in this phase.<sup>35</sup> The position of the Li atom is split into two equal parts, separated 0.9 Å long the hexagonal *c*-axis, enabling fast  $(\text{Li})^+$  hopping. Therefore, the ionic conductivity is primarily related to the hexagonal HT phase, offering these special positions not present in the LT phase. A stabilization of this phase by halide ions leads to an enhanced ion conductivity as compared to the LT orthorhombic phase of the pure system at the same temperature. The hexagonal HT structure is also responsible for the rapid reorientation of the  $(\text{BH}_4)^-$  anions. Potential energy surface maps reveal a more shallow potential for the  $(\text{BH}_4)^-$  as compared to the LT phase, lower energy barriers, and the absence of localized minima.<sup>3</sup> Consequently, the frequency of rotational jumps of the  $(\text{BH}_4)^-$  ion is higher than in the LT phase. The concurrent occurrence of enhanced anion reorientation and fast ion conduction in  $\text{LiBH}_4$  and in  $\text{LiBH}_4/\text{LiI}$  solid solutions does not necessarily imply that one is the cause of the other. Both are a consequence of the structural phase transition. However, the rotational freedom of the  $(\text{BH}_4)^-$  may have an influence on the Li diffusivity.

Fast Li ion conductivity has been observed in the HT phases of other ionic compounds with rotating complex anions. The rotation of the anion might support the cation diffusion by the so-called paddle wheel mechanism.<sup>12</sup> Also, in the case of  $\text{LiBH}_4$ , the fast  $(\text{Li})^+$  conduction only appears in the HT phase and is

accompanied by rapid reorientations of the complex anion. Stabilizing the HT phase by iodide substitution also leads to the increase of ionic conductivity and, at the same time, to an increase in reorientational motion of the  $(\text{BH}_4)^-$ .

According to Ikeshoji et al, the orientational freedom of the  $(\text{BH}_4)^-$  allows one to satisfy the tridentate relation, in which three H of the  $(\text{BH}_4)$  face the nearest Li neighbor.<sup>35</sup> As the negative charge of the  $(\text{BH}_4)^-$  is located on the H, this is the electrostatically most favorable situation. A  $(\text{Li})^+$  jump causes the surrounding  $(\text{BH}_4)^-$  to adjust their orientation accordingly. In other words,  $(\text{Li})^+$  and  $(\text{BH}_4)^-$  move jointly together. High barriers for the rotational motion of the  $(\text{BH}_4)^-$  hinder this adjustment and consequently reduce the  $(\text{Li})^+$  conductivity. For the  $(\text{I})^-$ , which has a more spherical charge distribution, the orientation of the ion toward the Li does not play a role. In short, due to the nonspherical structure of the  $(\text{BH}_4)^-$  anion, hopping of Li-ions is sterically hindered.

Ions such as  $(\text{I})^-$  have a spherical charge distribution, and thus their rotation does not influence the hopping of the Li-ion. Furthermore, also the rotational movement of the  $(\text{BH}_4)^-$  anions themselves is sterically hindered by the neighbor  $(\text{BH}_4)^-$  anions. Exchanging them by spherical anions helps in enhancing the rotational diffusion as experimentally observed. A direct proof of the influence of the number of anions/pseudoanions is given by Raman spectroscopy.<sup>37</sup> The shift of the stretching vibrations toward lower energies is a clear indication of a reduced coupling between the  $(\text{BH}_4)^-$  anions, observed upon the increase of either temperature or  $(\text{I})^-$ -concentration, respectively.

#### ■ AUTHOR INFORMATION

##### Corresponding Author

\*E-mail: pascal.martelli@empa.ch.

#### ■ ACKNOWLEDGMENT

This work is based on experiments performed at the Swiss spallation neutron source SINQ, Paul Scherrer Institute, Villigen, Switzerland.

We are thankful for the financial support from the Swiss National Science Foundation (SNF-Projects 200021-119972/1 and 200020-134442/1).

#### ■ REFERENCES

- (1) Züttel, A.; Rentsch, S.; Fischer, P.; Wenger, P.; Sudan, P.; Mauron, Ph.; Emmenegger, Ch. Hydrogen storage properties of  $\text{LiBH}_4$ . *J. Alloys Compd.* **2003**, 356, 515–520.
- (2) Züttel, A.; Borgschulte, A.; Orimo, S. I. Tetrahydroborates as new hydrogen storage materials. *Scr. Mater.* **2007**, 56, 823–828.
- (3) Buchter, F.; Lodziana, Z.; Mauron, Ph.; Remhof, A.; Friedrichs, O.; Borgschulte, A.; Züttel, A.; Sheptyakov, D.; Strassle, Th.; Ramirez-Cuesta, A. J. Dynamical properties and temperature induced molecular disordering of  $\text{LiBH}_4$  and  $\text{LiBD}_4$ . *Phys. Rev. B* **2008**, 78, 094302.
- (4) Hartman, M. R.; Rush, J. J.; Udovic, T. J.; Bowman, R. C.; Hwang, S. J. Structure and vibrational dynamics of isotopically labeled lithium borohydride using neutron diffraction and spectroscopy. *J. Solid State Chem.* **2007**, 180, 1298–1305.
- (5) Soulié, J. Ph.; Renaudin, G.; Cerný, R.; Yvon, K. Lithium borohydride  $\text{LiBH}_4$ : I. Crystal structure. *J. Alloys Compd.* **2002**, 346, 200–205.
- (6) Remhof, A.; Lodziana, Z.; Martelli, P.; Friedrichs, O.; Züttel, A.; Skripov, A. V.; Embs, J. P.; Strässle, T. Rotational motion of  $\text{BH}_4$  units in  $\text{MBH}_4$  ( $M=\text{Li,Na,K}$ ) from quasielastic neutron scattering and density functional calculations. *Phys. Rev. B* **2010**, 81, 214304.

- (7) Maekawa, H.; Matsuo, M.; Takamura, H.; Ando, M.; Noda, Y.; Karahashi, T.; Orimo, S.-i. Halide-stabilized  $\text{LiBH}_4$ , a room-temperature lithium fast-ion conductor. *J. Am. Chem. Soc.* **2009**, *131*, 894–895.
- (8) Matsuo, M.; Nakamori, Y.; Orimo, S.; Maekawa, H.; Takamura, H. Lithium superionic conduction in lithium borohydride accompanied by structural transition. *Appl. Phys. Lett.* **2007**, *91*, 224103.
- (9) Callear, S. K.; Nickels, E. A.; Jones, M. O.; Matsuo, M.; Orimo, S. I.; Edwards, P. P.; David, W. I. F. Order and disorder in lithium tetrahydroborate. *J. Mater. Sci.* **2011**, *46*, 566–569.
- (10) Matsuo, M.; Sato, T.; Miura, Y.; Oguchi, H.; Zhou, Y.; Maekawa, H.; Takamura, H.; Orimo, S. Synthesis and lithium fast-ion conductivity of a new complex hydride  $\text{Li}_3(\text{NH}_2)_2\text{I}$  with double-layered structure. *Chem. Mater.* **2010**, *22*, 2702.
- (11) Lunden, A.; Mellander, B. E.; Bengtzelius, A.; Ljungmark, H.; Tarneberg, R. Electrical-conductivity, self-diffusion and phase-diagram of lithium-sulfate lithium-chloride and lithium-sulfate lithium bromide. *Solid State Ionics* **1986**, *18–9*, 514–518.
- (12) Lunden, A. On the paddle-wheel mechanism for cation conduction in lithium sulphate. *Z. Naturforsch., A: Phys. Sci.* **1995**, *50*, 1067–1076.
- (13) Secco, E. A. Ion-transport in sulfates-Percolation mechanism versus paddle-wheel mechanism. *Solid State Commun.* **1988**, *66*, 921–923.
- (14) Borucka, A. Z.; Bockris, J. O.; Kitchener, J. A. Self-diffusion in molten sodium chloride, a test of the applicability of the Nernst-Einstein equation. *Proc. R. Soc. London* **1957**, *241*, 554–567.
- (15) Borgschulte, A.; Gremaud, R.; Züttel, A.; Martelli, P.; Remhof, A.; Ramirez-Cuesta, A. J.; Refson, K.; Bardaji, E. G.; Lohstroh, W.; Fichtner, M.; Hagemann, H.; Ernst, M. Experimental evidence of librational vibrations determining the stability of calcium borohydride. *Phys. Rev. B* **2011**, *83*, 024102.
- (16) Karahashi, T.; Kumatani, N.; Noda, Y.; Ando, M.; Takamura, H.; Matsuo, M.; Orimo, S.; Maekawa, H. Room temperature lithium fast-ion conduction and phase relationship of  $\text{LiI}$  stabilized  $\text{LiBH}_4$ . *Solid State Ionics* **2011**, DOI:10.1016/j.ssi.2010.05.017.
- (17) Martelli, P.; Remhof, A.; Borgschulte, A.; Mauron, Ph.; Wallacher, D.; Kemner, E.; Russina, M.; Pendolino, F.; Züttel, A.  $\text{BH}_4^-$  self-diffusion in liquid  $\text{LiBH}_4$ . *J. Phys. Chem. A* **2010**, *114*, 10117–10121.
- (18) Oguchi, H.; Matsuo, M.; Hummelshoj, J. S.; Vegge, T.; Norskov, J. K.; Sato, T.; Miura, Y.; Takamura, H.; Maekawa, H.; Orimo, S. Experimental and computational studies on structural transitions in the  $\text{LiBH}_4$ - $\text{LiI}$  pseudobinary system. *Appl. Phys. Lett.* **2009**, *94*, 3.
- (19) Mesot, J.; Janssen, S.; Holitzner, L.; Hempelmann, R. FOCUS: Project of a space and time focussing time-of-flight spectrometer for cold neutrons at the Spallation Source SINQ of the Paul Scherrer Institute. *J. Neutron Res.* **1996**, *3*, 293–310.
- (20) Janssen, S.; Mesot, J.; Holitzner, L.; Furrer, A.; Hempelmann, R. FOCUS: A hybrid TOF-spectrometer at SINQ. *Phys. B (Amsterdam, Neth.)* **1997**, *234–236*, 1174–1176.
- (21) Hempelmann, R. *Quasielastic Neutron Scattering and Solid State Diffusion*; Oxford University Press: New York, 2000.
- (22) Bée, M. *Quasielastic Neutron Scattering*; Adam Hilger: Philadelphia, PA, 1988.
- (23) Blanchard, D.; Riktor, M. D.; Maronsson, J. B.; Jacobsen, H. S.; Kehres, J.; Sveinbjörnsson, D.; Bardaji, E.; Gil, Léon, A.; Juranyi, F.; Wuttke, J.; Hauback, B. C.; Fichtner, M.; Vegge, T. Hydrogen rotational and translational diffusion in calcium borohydride from quasielastic neutron scattering and DFT calculations. *J. Phys. Chem. C* **2010**, *114*, 20249.
- (24) Remhof, A.; Lodziana, Z.; Buchter, F.; Martelli, P.; Pendolino, F.; Friedrichs, O.; Züttel, A.; Embs, J. P. Rotational diffusion in  $\text{NaBH}_4$ . *J. Phys. Chem. C* **2009**, *113*, 16834–16837.
- (25) Filinchuk, Y.; Chernyshov, D.; Cerny, R. Lightest borohydride probed by synchrotron X-ray diffraction: Experiment calls for a new theoretical revision. *J. Phys. Chem. C* **2008**, *112*, 10579–10584.
- (26) Skripov, A. V.; Soloninin, A. V.; Filinchuk, Y.; Chernyshov, D. Nuclear magnetic resonance study of the rotational motion and the phase transition in  $\text{LiBH}_4$ . *J. Phys. Chem. C* **2008**, *112*, 18701–18705.
- (27) Verdal, N.; Hartman, M. R.; Jenkins, T.; DeVries, D. J.; Rush, J. J.; Udovic, T. J. Reorientational dynamics of  $\text{NaBH}_4$  and  $\text{KBH}_4$ . *J. Phys. Chem. C* **2010**, *114*, 10027–10033.
- (28) Barnes, J. D. Inelastic neutron scattering study of the “rotator” phase transition in n-nonadecane. *J. Chem. Phys.* **1973**, *58*, 5193–5201.
- (29) Lechner, R. E.; Badurek, G.; Dianoux, A. J.; Hervet, H.; Volino, F. On the rotational motion of the ammonium ion in the CsCl-type phase of  $\text{NH}_4\text{Br}$ : Results from quasielastic neutron scattering. *J. Chem. Phys.* **1980**, *73*, 934.
- (30) Hagemann, H.; Gomes, S.; Renaudin, G.; Yvon, K. Raman studies of reorientation motions of  $(\text{BH}_4)^-$  anions in alkali borohydrides. *J. Alloys Compd.* **2004**, *363*, 129–132.
- (31) Tomkinson, J.; Waddington, T. C. Inelastic neutron scattering from the alkali metal borohydrides and calcium borohydride. *J. Chem. Soc., Faraday Trans. 2* **1976**, *72*, 528–538.
- (32) Elliott, S. R. *Physics of Amorphous Materials*; Harlow: Essex, 1990.
- (33) Parisi, G. On the origin of the boson peak. *J. Phys.: Condens. Matter* **2003**, *15*, S765.
- (34) Borgschulte, A.; Jain, A.; Ramirez-Cuesta, A. J.; Martelli, P.; Remhof, A.; Friedrichs, O.; Gremaud, R.; Züttel, A. Mobility and dynamics in the complex hydrides  $\text{LiAlH}_4$  and  $\text{LiBH}_4$ . *Faraday Discuss.*, *151*, **2011**, paper 10, DOI: 10.1039/c0fd00011f.
- (35) Ikeshoji, T.; Tsuchida, E.; Ikeda, K.; Matsuo, M.; Li, H. W.; Kawazoe, Y.; Orimo, S. I. Diffuse and doubly split atom occupation in hexagonal  $\text{LiBH}_4$ . *Appl. Phys. Lett.* **2009**, *95*, 221901–3.
- (36) Arnbjerg, L. M.; Ravnsbæk, D. B.; Filinchuk, Y.; Vang, R. T.; Cerenius, Y.; Besenbacher, F.; Jørgensen, J.-E.; Jakobsen, H. J.; Jensen, T. R. Structure and dynamics for  $\text{LiBH}_4$ - $\text{LiCl}$  solid solutions. *Chem. Mater.* **2009**, *21*, 5772–5782.
- (37) Borgschulte, A.; Gremaud, R.; Kato, S.; Stadie, N. P.; Remhof, A.; Züttel, A.; Matsuo, M.; Orimo, S. I. Anharmonicity in  $\text{LiBH}_4$ - $\text{LiI}$  induced by anion exchange and temperature. *Appl. Phys. Lett.* **2010**, *97*.